

# Spatially Patterned Polymer Dispersed Liquid Crystals for Image-Integrated Smart Windows

Waqas Kamal, Mengmeng Li, Jia-De Lin, Ellis Parry, Yihan Jin, Steve J. Elston, Alfonso A. Castrejón-Pita, and Stephen M. Morris\*

Conventional polymer dispersed liquid crystal (PDLC) films have been successful as electrically-switchable screens for privacy applications. However, spatial patterning of the films so as to generate a visually appealing design, logo, or image typically requires intricate fabrication processes, such as the use of prefabricated photomasks that do not allow for on-demand designs. Herein is reported on the fabrication and characterization of spatially patterned PDLC “pixels” using drop-on-demand inkjet printing, and it is demonstrated how these materials can be used to form a new generation of smart windows that consist of embedded images or company logos, which can be made to disappear with the application of a voltage. Following refinements to the material rheology and the subsequent successful deposition of individual PDLC droplets, arrays of PDLC pixels are printed at a resolution of 250 pixels per inch with an individual pixel size of  $130\ \mu\text{m}$  operating at an electric field strength ( $E$ ) of  $E = 1.4\ \text{V}\ \mu\text{m}^{-1}$ . Finally, using the approach developed herein, these printed PDLC pixels are arranged to form a college emblem that is embedded within a smart window that can be made to disappear with the application of a voltage.

be switched between an opaque and transparent state with the application of a voltage. Furthermore, their compatibility with cost-effective production processes such as roll-to-roll processing has ensured their successful deployment as a “smart window” technology. In contrast to multilayered electrochromic devices, PDLC technology is typically based upon a single-layered film that consists of liquid crystal (LC) droplets suspended in a polymer matrix.<sup>[6–8]</sup>

The most common process employed to manufacture PDLC films involves the phase separation of a homogeneous mixture of LC and prepolymer, typically through a photopolymerization-induced phase separation technique (PIPS). This process can be used to form large area PDLCs films, which typically allows for a wide degree of control over droplet size and shape when compared to emulsification or thermal/solvent-induced phase separation techniques.<sup>[9–12]</sup> For smart

glass and window applications, the size of the LC droplet after phase separation is generally within the range of  $1\text{--}20\ \mu\text{m}$ .<sup>[13,14]</sup> These LC droplets lack any preferential macroscopic orientation between LC domains. By matching the refractive index of the polymer matrix to one of the refractive indices of the LC, typically the ordinary refractive index, then a transparent state can be obtained by reorienting the LC director with an applied electric field so that the refractive indices of the LC droplets and the polymer binder match.<sup>[11,15]</sup> Even though the PIPS technique provides flexibility in terms of the phase separation process, a drawback lies in the inherent homogeneity that results from the mixing and coating procedures, which produces films consisting of a single LC and polymer formulation. To obtain PDLC films with spatially varying properties, the photopolymerization process has to be performed with the aid of a photomask or hologram to create patterns or variations in the film morphology.<sup>[16,17]</sup>

Patterned PDLCs have attracted interest in recent years and several attempts have been made to manufacture them. Among the fabrication processes reported, irradiation of the material with coherent light allows for the use of holographic masks, which enables light with a structured intensity to be applied to the films.<sup>[17–20]</sup> Additionally, if the LC host is doped with an azo dye the use of a linearly polarized light source during the photopolymerization process can cause the LC director to adopt a preferential microscopic orientation following phase separation and the formation of a polymer binder.<sup>[21,22]</sup> Another method


## 1. Introduction

Polymer dispersed liquid crystals (PDLCs) belong to a class of electro-optic materials that have found application in a wide range of technologies including optical switches, light shutters, holographic gratings and, most notably, as electrically switchable privacy windows.<sup>[1–5]</sup> In the latter case, it is well known that PDLCs can be employed as an electrically-switchable alternative to conventional blinds or curtains as they can

W. Kamal, M. Li, E. Parry, Y. Jin, S. J. Elston, A. A. Castrejón-Pita, S. M. Morris

Department of Engineering Science  
University of Oxford  
Parks Road, Oxford OX1 3PJ, UK  
E-mail: stephen.morris@eng.ox.ac.uk

J.-D. Lin  
Department of Opto-Electronic Engineering  
National Dong Hwa University (NDHU)  
No. 1, Sec. 2, Da Hsueh Road, Hualien 974, Taiwan

 The ORCID identification number(s) for the author(s) of this article can be found under <https://doi.org/10.1002/adom.202101748>.

© 2021 The Authors. Advanced Optical Materials published by Wiley-VCH GmbH. This is an open access article under the terms of the Creative Commons Attribution License, which permits use, distribution and reproduction in any medium, provided the original work is properly cited.

DOI: 10.1002/adom.202101748

that has been proposed for obtaining a patterned PDLC film involves the use of holographic photopolymerization where two laser beams generate an interference pattern within a homogeneous LC and prepolymer formulation resulting in the formation of separate polymer-rich and LC-rich domains.<sup>[23,24]</sup> Other methods reported for producing a patterned PDLC film include the use of high-power light-emitting diodes, photo-masks, chemically patterned substrates, and using mechanical stamping processes.<sup>[11,25,26]</sup> Such methods show a high degree of accuracy at the micro/nanoscale, although these techniques often require multiple additional processing steps and are not widely compatible with large-area PDLC films, particularly those that have spatially varying properties.

Drop-on-demand (DoD) inkjet printing, which is a form of additive manufacturing, is a digital fabrication process that allows for small volumes of a fluid to be deposited at well-defined locations on a substrate.<sup>[27–29]</sup> It has rapidly emerged as a scalable technique that allows for functional inks to be delivered to a substrate at high speeds and with a high degree of accuracy. Because of its benefits in terms of ease of processing, inkjet printing is now employed in a multitude of industries including displays, pharmaceuticals, bioengineering, and printed electronics.<sup>[30–35]</sup> As the printing technology continues to develop, the range of complex fluids that can be processed has increased greatly. For example, printing has already been employed with LC materials to develop monodisperse LC solutions, and optically-pumped thin-film lasers, as well as electrically and thermally tunable microlenses.<sup>[36–39]</sup>

Due to its versatility, DoD inkjet printing offers a unique platform for the manufacture of PDLC films. By printing an LC and UV-curable polymer ink, PDLC films with spatially patterned emblems and logos can be successfully manufactured. In this work, we show how DoD printing can be used to create patterned PDLC films and present results that demonstrate the satellite-free printing of an LC-prepolymer ink without jet break-up, along with the light scattering properties of the individual printed PDLC droplets. Finally, smart windows with printed emblems and logos are demonstrated, and we conclude with a discussion of the electro-optic and viewing angle characteristics of these smart windows.

## 2. Results and Discussion

### 2.1. The Concept

The inkjet printing of the PDLC ink formulation and the subsequent device assembly is illustrated in **Figure 1**. Figure 1a,b shows that the droplets of the PDLC ink are directly deposited from a piezo-driven print-head onto an Indium tin Oxide (ITO)-coated glass substrate. For the demonstration of the printing of PDLC logos/emblems, the crest for Exeter College (a constituent College within the University of Oxford) is printed by precisely jetting individual droplets onto the substrate, which is later followed by device assembly (the addition of a top glass superstrate) and ultraviolet light (UV) illumination to photopolymerize the polymer binder. The experimental details for printing the ink and the process used to fabricate the devices are discussed further in the Experimental Section. Figure 1c

provides a schematic of the patterned PDLC device architecture, which includes the ITO-coated glass, film spacers, and the printed PDLC droplets. The ultimate goal of this work is to demonstrate that DoD inkjet printing can be used to form intricate and sophisticated PDLC patterns so as to create pictorial representations of logos/emblems/motifs within the smart window. Figure 1d therefore illustrates the proof-of-concept in which the printed image can be switched from an opaque to a transparent state in the presence of an electric field.

For this work, the PDLC formulations consisted of the eutectic nematic LC mixture, E7 (Synthon Chemicals Ltd.), which was dispersed with a Norland Optical Adhesive (NOA65, Thorlabs) at a weight ratio of 1:1. The nematic LC was chosen because its material properties are well-characterized and documented, and importantly it has been shown to be compatible with DoD printing.<sup>[36,38,39]</sup> NOA65 was chosen because this forms a homogeneous mixture with the LC before illumination with UV light and it has been employed previously as the polymer binder in PDLC systems. The refractive indices of the ordinary ( $n_o$ ) and extraordinary ( $n_e$ ) refractive index of the LC and the polymer binder ( $n_p$ ) at room temperature and a wavelength of 633 nm are  $n_o = 1.52$ ,  $n_e = 1.74$ , and  $n_p = 1.52$ , respectively.<sup>[40]</sup> This means that  $n_o$  and  $n_p$  are matched ensuring that a transparent state is obtained when an electric field is applied so as to reorient the LC director within the array of microdroplets contained within each printed droplet. The combination of the nematic LC and the NOA65 prepolymer results in a mixture that is highly viscous and non-Newtonian. Therefore, the print-head temperature and voltage waveform parameters were varied so as to identify the conditions required in order that single droplets could be dispensed from the nozzle that were free of jet break-up or the formation of satellite droplets.

### 2.2. Printing the PDLC Ink

The dimensionless number  $Z$  (the inverse of the Ohnesorge number) can serve as a useful metric for the selection of the fluid for printing, which is defined as the ratio of the Reynolds number,  $R_e$  to the square root of the Weber number  $W_e$ .<sup>[41]</sup> This can be written as

$$Z = \frac{R_e}{\sqrt{W_e}} = \frac{\sqrt{\gamma \rho d}}{\mu} \quad (1)$$

where  $\gamma$ ,  $\rho$ ,  $\mu$  are the surface tension, density, and viscosity of the ink, respectively, and  $d$  is a characteristic length, which can be the diameter of the jet, nozzle, or drop. Studies have shown that a value of  $1 < Z < 10$  is typically required to eject a well-formed single drop without the formation of single or multiple satellite droplets.<sup>[41,42]</sup> The PDLC ink exhibits a temperature-dependent viscosity and surface tension, and measurements of these properties at different temperatures are shown in Figure S1 and Table S1 (see the Supporting Information and the Experimental Section). At 70 °C the bulk viscosity and surface tension are found to be reduced from 811.31 mPa s and 36.1 mN m<sup>−1</sup> at room temperature to 25.4 mPa s and 31.2 mN m<sup>−1</sup>, respectively. These reduced material parameters at elevated temperatures are found to be compatible with the inkjet printing process, as discussed below.

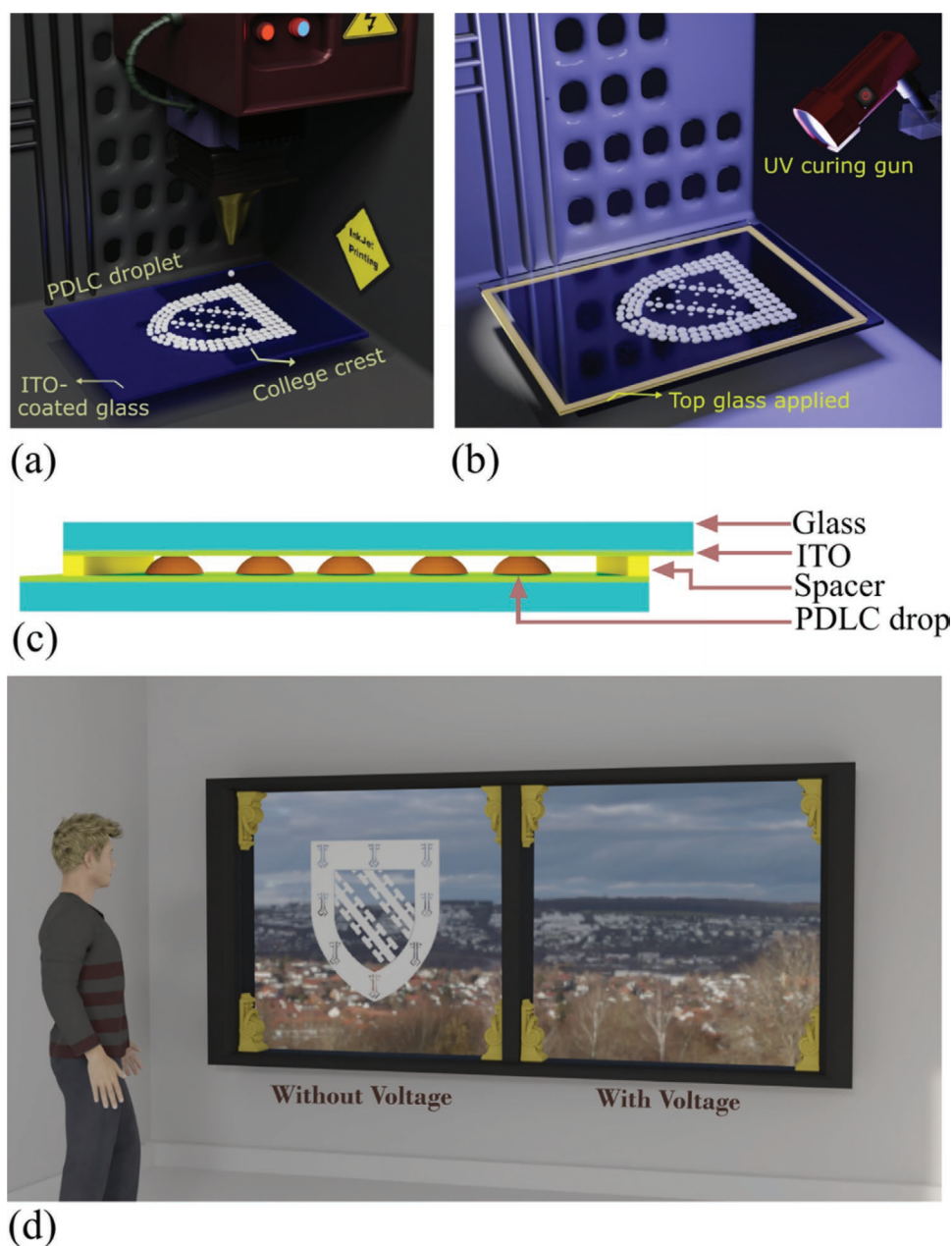


**Figure 1.** a) Illustration of the use of drop-on-demand inkjet printing for precision-patterned polymer dispersed liquid crystal (PDLC) inks on a glass substrate. b) Illustration showing the addition of the top glass superstrate and the illumination of the sample using ultraviolet light so as to form the polymer binder in each of the separate printed PDLC “pixels.” c) Schematic diagram showing a side view of the resulting device stack. d) A graphical representation of the printed PDLC smart glass concept in which a company logo or emblem can be made to disappear with the application of an electric field.

To reduce the bulk viscosity and surface tension, the print head temperature was increased, and the input waveform adjusted so as to generate a satellite-free droplet. As an example, **Figure 2a** shows the in-flight motion of a single droplet which could be reliably generated during one jetting cycle. During flight, the observed drop diameter was found to be  $65 \pm 5 \mu\text{m}$  and the droplet volume was  $180 \pm 30 \text{ pL}$ . The corresponding drop velocity during this cycle was  $1.38 \text{ ms}^{-1}$ ; these combined fluid properties indicate that this is well below the point at which splashing may occur.<sup>[43]</sup> As presented in the plot of Weber number as a function of the Reynolds number

(Figure 2b), this is found to correspond to a Z number of 2.04, which is within the range consistent with satellite-free printing. **Table 1** lists the dimensionless PDLC ink fluid properties for the printing conditions used here. It should be noted that at a temperature of  $20^\circ\text{C}$  the PDLC ink was very viscous, and the corresponding Z number was found to be 0.16, which is too viscous to print. Hence, printing was performed at an elevated temperature of  $T = 67^\circ\text{C}$ .

The drop speed can be increased by varying the amplitude of the input waveform.<sup>[44]</sup> Our printing setup allowed us to vary the drop velocity by changing the voltage amplitude of the

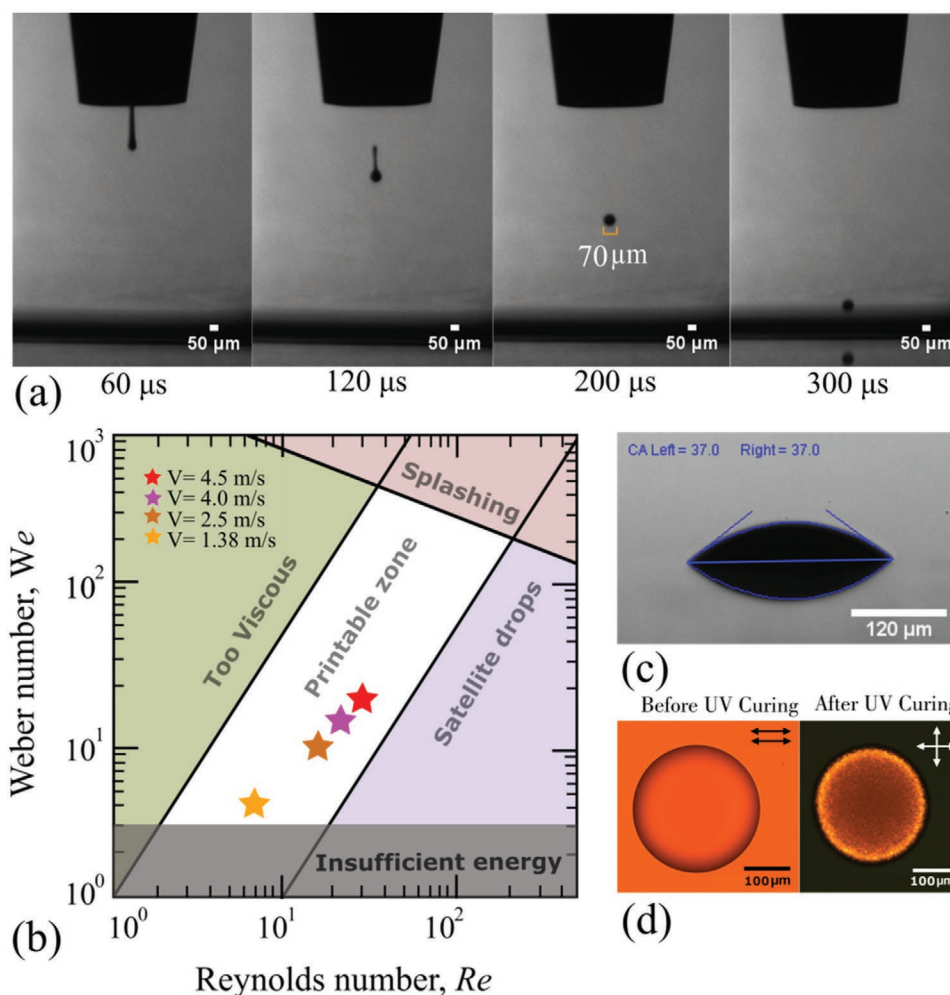


**Figure 2.** Drop-on-demand printing of polymer dispersed liquid crystal (PDLC) droplets. a) Shadowgraphy images showing the deposition of a PDLC ink formulation (50 wt% NOA65 + 50 wt% E7) at a temperature of 67° over a timescale from 60 μs (just after ejection) to 300 μs (just before impact with the substrate surface). The ink was ejected from an 80 μm diameter MicroFab nozzle. The printing is performed with a unipolar trapezoidal waveform with 3, 15, and 4 μs rise, dwell and fall times, respectively. The dwell voltage was 90 V, which was varied from 90 to 110 V so as to form a stable droplet at different ejection velocities. b) Parameter map showing the Reynolds and Weber numbers of the PDLC ink at a temperature of 70°. The stars correspond to the velocities at which no satellites were observed, confirming the printable regime. c) Shadowgraph image of a PDLC droplet with a  $37^\circ \pm 2^\circ$  contact angle that has been formed by depositing 5 droplets onto the same location of the substrate. The approximate height of the droplet was found to be  $30 \pm 5$  μm and the droplet diameter was  $230 \pm 5$  μm. The image was taken  $\approx 4$  min after the deposition of the drop and before the UV illumination process. d) Polarized optical microscope images before and after UV curing. The first image was captured before UV curing and was taken in the presence of a UV filter fitted to the microscope. The image was taken around 10 min after the printing process. The two black double-headed arrows correspond to the transmission axes of the analyzer and polarizer, which were parallel to each other. Similarly, for the second image, which was taken after the UV illumination process, the two white double-headed arrows correspond to the transmission axes of the analyzer and polarizer being perpendicular to each other.

waveform between 90 and 110 V, which controlled the drop velocity to be in the range of 1.38 and 4.5 ms<sup>-1</sup>. However, it was found that above a drop velocity of 4.5 ms<sup>-1</sup>, a spontaneous

**Table 1.** Dimensionless fluid properties for the printing conditions used here.

Drop velocity [m s <sup>-1</sup> ]	$Re$	$We$	$Z$
1.38	4.700 017	5.28	2.04
2.5	8.514 524	17.3	2.04
4	13.62 324	44.37	2.04
4.5	15.32 614	56.16	2.04

break-up of the fluid ligament was observed which resulted in the formation of satellite droplets. Therefore, the waveform conditions were adjusted such that the droplet velocity was always less than 4.5 ms<sup>-1</sup> so as to avoid the formation of satellite droplets that accompany the main printed droplet.

Before building the device structure illustrated in Figure 1, droplets were first printed onto a single ITO-coated glass substrate. By adjusting the input waveform, it is possible to make small changes to the drop volume of an individual PDLC droplet deposited on a substrate. However, a subtle change in back pressure can also lead to printing instabilities. To circumvent the issue of potential printing instabilities, the droplet volume was increased by landing multiple drops onto the same position of the substrate. To demonstrate this, both single and



multiple droplets were deposited to form PDLC “pixels.” As an example, Figure 2c,d presents results of the side profile and polarized optical microscopy images, respectively, of a PDLC pixel formed by landing 5 droplets of the ink onto the same location of the substrate, which is discussed in more detail shortly. Examples of single droplet pixels are presented later in the manuscript.

The morphology of a PDLC pixel was analyzed using calibrated polarized optical microscopy and shadowgraphy images. The PDLC pixel deposited onto an ITO-coated glass substrate was found to reach an equilibrium state within a few milliseconds where it attains a spherical cap shape with a contact angle of  $37^\circ \pm 2^\circ$ , as shown in Figure 2c. The contact angle does not depend upon pixel volume, as verified for 7 different variable size pixels, which were all found to be  $37^\circ \pm 2^\circ$  in each case (see Figure S2, Supporting Information). Figure 2d shows polarizing optical microscope images of a printed PDLC droplet before and after the UV curing process. To inspect the printed droplet immediately after the printing process, and in order to prevent any unwanted polymerization of the prepolymer from taking place, the first microscope image in Figure 2d was taken with a filter fitted to the microscope that blocks UV light. The example image that was obtained (transmission axes of the polarizer and analyzer aligned parallel to each other) confirms that the LC and prepolymer mixture did not appear to phase separate during or after the printing process. Phase separation was only found to take place after the UV illumination process. The second image in Figure 2d shows a crossed polarized microscope image of the printed PDLC droplet after the UV illumination process, where it can be seen that the droplet strongly scatters the light when it is illuminated with a microscope halogen light source. Note that during the printing process only the print head was at the elevated temperature—the substrate temperature and the temperature during the device assembly and photopolymerization processes were maintained at room temperature, as is common in PDLC device manufacture. However, it was necessary to elevate the print-head temperature in order to control and optimize the PDLC ink properties for printing.

### 2.3. Electro-Optic Characteristics of a Printed PDLC Droplet

To evaluate the ability of an array of PDLC droplets to switch between transparent and opaque states, the electro-optic behavior for a single PDLC droplet was first characterized using a high numerical aperture objective lens on an optical polarizing microscope operated in a transmission mode. To do this, a top electrode was added before the printed PDLC droplet was polymerized using UV illumination, as illustrated in Figure 1c. For the printed PDLC droplets to switch from a scattering (voltage OFF) state to a transparent (voltage ON) state, the LC director must reorient under the application of an electric field. When the LC director is oriented along the direction of an applied electric field (for the case of a positive dielectric anisotropy nematic LC), the incident light will experience only the ordinary component of the LC refractive index ( $n_o = 1.52$ ). Since this is closely matched to the refractive index of the cured photopolymer ( $n_p = 1.52$ ), the incident light is then not scattered by the pixel as illustrated schematically in Figure 3a.

Figure 3b presents results for a  $230 \pm 5 \mu\text{m}$  diameter PDLC droplet at a range of voltage amplitudes for a 1 kHz frequency square wave. It is obvious from the image sequence that in the OFF state ( $0 V_{pp}$ ) the PDLC pixel appears opaque and strongly scatters the incoming light from the microscope lamp. However, upon the application of an electric field the director in the LC domains begins to align along the direction of the applied field, and the PDLC droplet gradually becomes transparent, as shown in the images. It was found that there was some variation in the switching of the LC domains due to the variation in the height of the droplet which results from the curved shape. The device thickness, however, was a constant value and found to be  $28 \pm 1 \mu\text{m}$ . From the line profile in Figure 3c and the polarizing optical microscope images in Figure 3b, it can be seen that a bright ring initially appears inside the periphery of the PDLC droplet when the voltage amplitude is between 10 and  $20 V_{pp}$ , and the corresponding electric field strength ( $E$ ) ranges from  $E = 0.18 \text{ V } \mu\text{m}^{-1}$  to  $E = 0.36 \text{ V } \mu\text{m}^{-1}$ . A further increase in the electric field amplitude causes the LC domains at the center of the droplet to switch before the remainder of the droplet becomes transparent. It can be seen in Figure 3b,c that at  $100 V_{pp}$  ( $E = 1.8 \text{ V } \mu\text{m}^{-1}$ ) all of the LC domains in the centre and periphery of the droplet are switched to the ON (transparent) state, although a small degree of scattering can still be observed in the central region of the droplet.

At normal incidence, the scattering of light from a printed PDLC droplet was observed to determine the scattering behavior of the LC domains at a range of angles. For this characterization, the droplet was illuminated with a continuous wave He–Ne laser. The angular distribution of the scattered light intensity was measured with the experimental system shown schematically in Figure S3 (Supporting Information). A photodiode and collection lens mounted on a rotation stage were rotated between  $-45^\circ$  and  $+45^\circ$ . For each angle, the scattered light received by the detector was recorded and the results are presented in Figure 3d. The graph shows that scattered intensity is nonuniform with angle, and it tends to decrease when the photodiode collecting the scattered light reaches the extreme angles (i.e.,  $-45^\circ$  to  $+45^\circ$ ). However, the variation in the scattered intensity is almost identical on either side of  $0^\circ$  indicating that the LC domains inside the printed droplet are relatively uniformly distributed within the polymer binder. Knowledge of the angular distribution of the scattered light from the printed PDLC droplets is of importance for applications, such as smart windows where the distribution of light scattered by a printed PDLC droplet determines the fraction of incident solar energy passing through it. For printed logos or emblems, the angular scattering determines how well the logo/emblem can be seen over a range of angles.

Further, quantitative measurements for the optical transmission of the same PDLC droplet was performed using the setup shown in Figure S3 (see the Supporting Information and the Experimental Section). Figure 3e shows the resulting optical transmission through the printed PDLC droplet. For these measurements, a 1 kHz applied voltage was ramped up from 0 to  $200 V_{pp}$  over a timescale of 6.66 s. Laser light from a He–Ne laser was focused onto a printed PDLC “pixel” using a lens. Two separate photodiodes were used to capture the transmitted and scattered light from the printed PDLC droplet simultaneously.

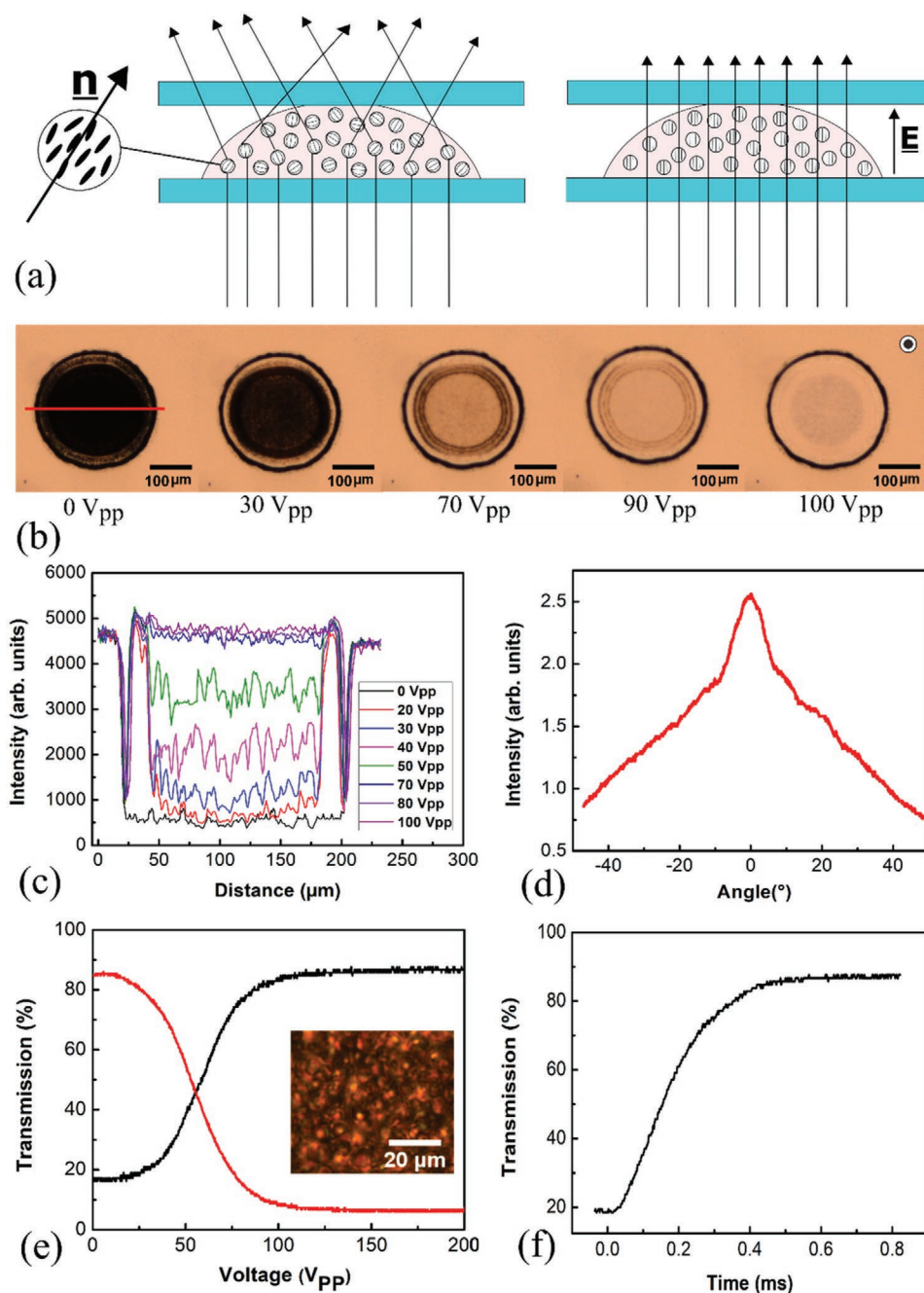


**Figure 3.** a) Schematic representation of a PDLC pixel consisting of micrometer-sized LC droplets. The unit vector  $n$  represents the alignment of the nematic director for an individual droplet. b) Optical polarized microscope images of a  $230 \pm 5 \mu\text{m}$  printed PDLC droplet (50 wt% NOA65 + 50 wt% E7) when subjected to an electric field of different amplitudes. The white circle in the top right corresponds to the direction of the applied electric field, which is out of the plane of the device. Prior to the application of an electric field, a top electrode was fitted resulting in a device thickness of  $28 \mu\text{m}$  between the top and bottom electrodes. Following this, the entire sample was irradiated with UV light ( $365 \text{ nm}$ ) at a power density of  $65 \text{ mW cm}^{-2}$  for a duration of 4 min at room temperature. c) Line profile plots extracted from the microscope image of the printed PDLC droplet at different voltages. The data were recorded using an Olympus BX51 microscope fitted with a  $10\times$  objective lens. d) The angular dependence of the scattered light for a single PDLC droplet in the voltage OFF (opaque) state. e) Transmission as a function of voltage of the PDLC droplet presented in b). The black and red lines represent the change in the intensity of the transmitted and back scattered light, respectively. Inset shows an optical polarizing microscope image of a section of the PDLC droplet revealing LC domain sizes in the range of 5–6  $\mu\text{m}$ . f) Response (rise) time of the droplet captured for the scattered light component.

The results show that the transmission started to increase with the applied voltage before reaching a maximum at  $100 \text{ V}_{\text{pp}}$ , while at the same time the scattered light reduces

with increasing voltage before reaching a minimum value at the same applied voltage of  $100 \text{ V}_{\text{pp}}$ . For an illumination wavelength of  $\lambda = 632.8 \text{ nm}$  and at  $0 \text{ V}_{\text{pp}}$ , the transmission is found

to be 19% which increases to 85% at 100 V<sub>pp</sub>. The threshold voltage  $V_{th}$ , and saturation voltage  $V_{sat}$ , defined as the applied voltage amplitude at which 10% and 90% of the possible transmission range is achieved, respectively, were found to be  $V_{th}=38$  V<sub>pp</sub> and  $V_{sat}=64$  V<sub>pp</sub>. In terms of electric fields strengths, this corresponds to  $E_{th}=0.7$  V  $\mu\text{m}^{-1}$  and  $E_{sat}=1.15$  V  $\mu\text{m}^{-1}$ . The printed PDLC droplet was further investigated to determine the contrast ratio, which is usually characterized by the ratio of transmittance values of a transparent to an opaque state. The contrast ratio,  $CR = T_{on}(\%)/T_{off}(\%)$ , is a ratio of maximum to minimum transmittance of a PDLC device, and the CR value of a printed PDLC droplet here was 4.4, which is similar to conventional photocurable polymer-based PDLC film technologies.<sup>[45,46]</sup>

The difference in transmission is comparable to observations reported previously on PDLC films of a similar film thickness that have been targeted for use in smart window technologies.<sup>[15,45,47]</sup> The dynamic response of the PDLC domains to an applied electric field is also an important device parameter for many applications, such as in light shutters. The rise time,  $t_{rise}$ , and decay time  $t_{decay}$  in this study is defined as the time in which the film transmittance changes from 10% to 90%, and from 90% to 10%, respectively. To characterize the PDLC pixels in terms of their dynamic response, the optical setup shown in Figure S3 (Supporting Information) was employed. For this, a 1 kHz square wave of 200 V<sub>pp</sub> was periodically modulated to turn on and off at a frequency of 150 mHz. The results for the rise and decay times are presented in Figure 3f; and Figure S4 (Supporting Information), respectively. The results show that the switching ON time, from opaque to transparent state, and the switching OFF time, from transparent to opaque state, takes around  $t_{rise}=0.15$  ms and  $t_{decay}=77$  ms, respectively. The dynamic response time measurements of the printed PDLC droplet is found to be in good agreement with the results reported previously for conventional PDLC films and represent a timescale that is expected for LC domain sizes that are of the order of 5  $\mu\text{m}$ .<sup>[45,46]</sup>

## 2.4. Printed PDLC Arrays

An inkjet printer typically reads a digital image and then prints a defined density of droplets per unit length (defined as the “dots per inch = dpi”). After printing, each droplet forms a “pixel” and the density of the pixels in the resulting device can be considered analogous to the dpi settings of the printer. For a printed PDLC technology, the scattering is an important parameter in terms of device performance and is dependent on the number of droplets deposited over a certain substrate area. For a fixed device thickness of  $\approx 14$   $\mu\text{m}$ , experiments were conducted to determine how closely the individual droplets could be printed before they were found to coalesce during the printing and device assembly stages. Note that in the following the device thickness has been reduced in order to decrease the voltage amplitude required to switch the PDLC “pixels” to a transparent state. Figure 4a; and Figure S5 (Supporting Information) shows microscope images of the droplets with a constant volume of 180 pL that were printed with 20, 40, and 50  $\mu\text{m}$  spacings between neighboring droplets. The droplet volume, and consequent pixel size, is dictated by the print head nozzle size used, which had a diameter of 80  $\mu\text{m}$ . Attempts to print

with a smaller nozzle of diameter 50  $\mu\text{m}$  were not successful due to the physical properties of the PDLC ink. Note that in order to adjust the droplet spacings the step sizes of the printer were varied. However, the minimum step size available with our system is 10  $\mu\text{m}$ , corresponding to a maximum effective resolution of 250 dpi for the image (although this is of course “blurred” by size of the individual printed droplets). After device assembly, the droplets were brought into direct contact with the top glass substrate, which resulted in a subtle increase in the droplet diameters. Nevertheless, each pixel remained circular in shape with a  $\pm 10$   $\mu\text{m}$  variation in the droplet diameter (see Figures S5 and S7, Supporting Information). There is also a small variation in terms of the contact of the top ITO electrode with the cap of some of the droplets as can be seen in the microscope images in Figure S5 (Supporting Information). This is believed to result from the application of an uneven amount of mechanical pressure during device fabrication when the top glass substrate was attached to the printed substrate.

The time taken to print a pattern depends upon drop ejection frequency and the substrate speed. In our pattern printing experiment, we set the print nozzle frequency to 1000 Hz and the substrate speed to 40 mm s<sup>-1</sup>. For a pattern with an area of 896 mm<sup>2</sup>, as shown in Figure 4b, the time taken to print this pattern was  $\approx 5$  min.

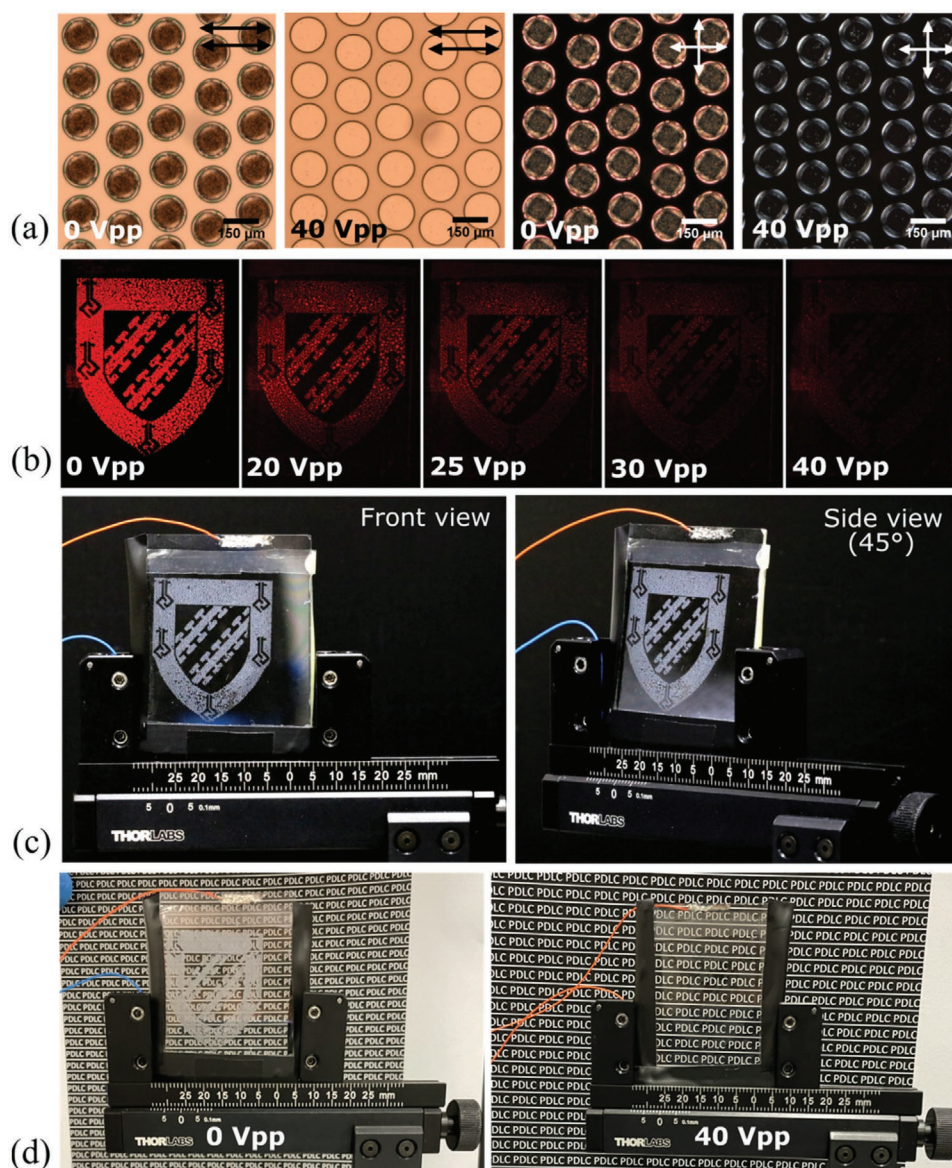
An attempt was made to print the droplets with spacings less than 15  $\mu\text{m}$ . However, for such small droplet spacings the uneven pressure applied during the application of the top glass substrate resulted in the droplets amalgamating and the printed PDLC then appeared similar in morphology to a conventional PDLC film rather than individual PDLC droplets, as shown in Figure S6 (Supporting Information). With droplet spacings in the range of 2–15  $\mu\text{m}$  the droplets were found to completely aggregate after device assembly, and with spacings of the order of 15–17  $\mu\text{m}$  partial aggregation with each other tends to take place. A droplet spacing of 20  $\mu\text{m}$  was found to be an optimal spacing to engineer coalesced-free individual droplets sandwiched between the top and bottom electrodes. For high-resolution printing, a spacing equivalent to the size of a single droplet is often employed in the literature.<sup>[48,49]</sup> Therefore, printing with highly viscous LC polymer composites to obtain a 130  $\mu\text{m}$  diameter PDLC pixel with a gap of less than one quarter of the pixel diameter ( $d$ ) is considered to be a successful demonstration of high resolution inkjet printing of a PDLC ink (i.e., a center to center printing spacing of 1.25d).

Figure 4a shows examples of polarized optical microscopy images of arrays of PDLC droplets switching under the application of an external electric field, where it can be seen that the PDLC pixels switch uniformly across the device. Crossed polarised microscope images for the OFF and ON states confirm that the droplets can be switched in unison from an opaque to a transparent state. If desired, multiple ink droplets dispensed onto the same location can be used to locally enlarge the PDLC “pixels” as can be seen in Figure 2a.

## 2.5. Printed PDLC Smart Window

To create a prototype electrically switchable PDLC smart window with embedded images, the printed PDLC “pixels”





**Figure 4.** a) Polarized optical microscope images of printed PDLC droplets at 0 and 40 V<sub>pp</sub>. The top right black double-headed arrows in the images indicate that the analyzer and polarizer axes are aligned parallel to one another. The white double-headed arrows that are crossed indicate that the transmission axes of the analyzer and polarizer are perpendicular to one another. The individual drop diameter is  $130 \pm 5 \mu\text{m}$  and the measured device thickness is  $14 \mu\text{m}$ . b) The crest illuminated with a halogen light source and images were recorded with a CCD camera. A square-wave of 1 kHz frequency was applied from 0 to 40 V<sub>pp</sub>. c) Photographs captured using a digital SLR camera at 0 V<sub>pp</sub> from the front and side views. d) The crest in front of the printed text on white paper to show the scattering and transmission at 0 and 40 V<sub>pp</sub> ( $E = 1.4 \text{ V } \mu\text{m}^{-1}$ ), respectively, when viewed at normal incidence.

were covered with a top glass substrate and subjected to UV illumination to form the polymer binder and LC domains in each droplet. Figure 4b,c demonstrates a prototype printed smart window displaying the Exeter College (Oxford) crest. The printed crest, as can be seen in Figure 4b, was illuminated with a halogen light source and a series of images were recorded for a range of voltages between the OFF state and the ON (transparent) state. The threshold voltage,  $V_{\text{th}}$ , and saturation voltage,  $V_{\text{sat}}$ , for this printed sample were found to be 9 and 32 V<sub>pp</sub>, respectively. In terms of electric fields strengths, this corresponds to  $E_{\text{th}} = 0.3 \text{ V } \mu\text{m}^{-1}$  and  $E_{\text{sat}} = 1.14 \text{ V } \mu\text{m}^{-1}$ . The complete switch ON electric field strength for which the device appears

transparent was found to be  $E = 1.4 \text{ V } \mu\text{m}^{-1}$ , which is comparable to that obtained for conventional PDLC film-based preparation techniques.<sup>[45]</sup>

Figure 4c shows images captured using a digital SLR camera of the printed Exeter College crest taken when viewed from the front and at an angle to the device. It can be seen that the printed crest strongly scatters light when viewed both at normal ( $0^\circ$ ) and at oblique ( $45^\circ$ ) viewing angles. Similarly, when in the ON state and viewed over the same range of angles the printed crest could not be seen as the device appears transparent (Figure S8, Supporting Information). To further illustrate the quality of the switching, scattering, and transparency, the crest



was switched ON and OFF above text printed onto white paper, as presented in Figure 4d. It is evident that the crest in the OFF state scatters the light and the text behind the device is completely hidden. In contrast, for the ON state, the crest disappeared and the text behind the device could be read clearly. These results suggest that the density of the printed droplets was sufficient to create a printed PDLC smart window with a switchable logo. Furthermore, the overall performance of the printed crest in terms of the light scattering, light transmittance, and contrast ratio was investigated by measuring the behaviour of individual pixels in regions within the printed pattern. It was found that the individual pixels in the printed pattern shown here have the same electro-optic properties as those presented in detail in Section 2.3 for an individual printed PDLC droplet.

### 3. Conclusion

In summary, we have demonstrated new patterned PDLC films that have been fabricated using a printing process and have shown that these printed materials could be used to form a smart window technology with logos and images that can be made to disappear with the application of a voltage. To begin with, the rheology and surface tension of the ink was tuned by varying the print-head temperature in order to eject uniform-sized droplets. PDLC droplets consisting of a high density of LC domains were formed upon irradiation of the sample with UV light. The photocuring conditions were chosen such that the droplets give rise to intense scattering of light leading to high quality arrays of PDLC “pixels.” We believe that the technique reported here is significant as it provides a means with which to pattern a PDLC film without the need for photomasks and would allow for different LC formulations to be used simultaneously on a substrate with the aid of a multiprinthead printing system. The approach described herein would allow for artistic designs, motifs, and additional information, such as dynamic company logos or advertisements to be displayed on smart windows that could be removed with an applied voltage. Further, there is considerable scope to enlarge the size of the printed patterns using commercial processes based on multi-nozzle printing over large area substrates. In addition, the flexibility of the process would allow the expansion of the smart windows manufacturing concept to roll-to-roll manufacturing by printing and assembling PDLC inks between flexible substrates on a production line system. The future scope for the commercial exploitation of the concepts introduced here is therefore substantial.

### 4. Experimental Section

**Materials and Ink Preparation:** For this study, the nematic LC mixture E7 (Synthon chemicals Ltd.) with refractive indices of  $n_o = 1.52$  and  $n_e = 1.74$  at  $\lambda = 633$  nm and  $20^\circ\text{C}$  was used as the LC component. The Norland Optical Adhesive, NOA65 (from Norland products) with a refractive index of  $n_p = 1.52$ , was used as the polymer binder.<sup>[40]</sup> The glue and LC were prepared as a 1:1 composition. The formulation was mixed over a hot-plate and stirred for 24 h at 300 rpm at  $65^\circ\text{C}$ . The temperature was chosen in order to raise the formulation above the

clearing temperature of the LC,  $T_c = 58^\circ\text{C}$  and to reduce the viscosity and surface tension.

**PDLC Device Fabrication:** ITO-coated glass substrates were cleaned with isopropyl alcohol and rinsed with deionized water before being sonicated for 20 min in acetone. The substrates were baked for 2 min to confirm that they were completely dry. The drop-on-demand inkjet printing of the PDLC ink on the prepared substrates was accomplished by using a commercially available printing system (Jetlab-II, MicroFab Technologies Inc.), which consists of a motorized stage and temperature-controlled print-heads. To print within an accuracy of  $\pm 5\ \mu\text{m}$ , an  $80\ \mu\text{m}$  diameter MicroFab dispenser was employed. The pressure of the print-head was adjusted using a computer-controlled pneumatic system to optimize the liquid flow and wetting of the nozzle-orifice. As the PDLC ink is highly viscous, the ink was raised to elevated temperatures to reduce its viscosity. Therefore, the print-head was heated to  $67^\circ\text{C}$  to bring the material into the isotropic phase resulting in a stable droplet generation from the nozzle (i.e., no jet or satellite droplet formation). The printing substrate was held at room temperature of  $\approx 20^\circ\text{C}$  for all the samples presented in this study.

A high-speed camera (Phantom V12.1) in a shadowgraphy configuration illuminated with an UV filtered halogen high-intensity white light source (OSL2 3200K, Thorlabs) was employed to observe drop generation and deposition on the substrate. After printing, spacer tape on both sides of the printed sample was placed to define an approximate device thickness. A top electrode was placed such that both ITO-coated surfaces faced each other in order to form a glass cell. The substrates were clamped down using two clamps to ensure an even pressure distribution across the cell. Following that, the substrates were fastened using a rapid epoxy adhesive (from Araldite) at room temperature. Finally, the device was photocured using an ultraviolet light ( $\lambda = 365$  nm) source (CS2010, Thorlabs) with power density of  $62.5\ \text{mW cm}^{-2}$  for 10 min, which was measured using a handheld power meter (PM100D, Thorlabs) attached to a photodiode (S120VC, Thorlabs). All of the above steps, including inkjet printing, were carried out under the illumination of yellow light until the sample was fully phase separated. For the application of an electric field, wires were connected to the ITO substrates using indium shot.

**Characterization:** The viscosity and surface tension of the PDLC ink were recorded by a Physica MCR301 rheometer (from Anton Paar) and bubble tensiometer (from SITA), respectively. The contact angle was measured by sessile droplet method using high speed camera frames (Phantom V12.1). The printed PDLC domain sizes, light scattering properties, and sizes were recorded using an Olympus BX51 optical polarizing microscope. The optical arrangement shown in Figure S4 (Supporting Information) was used to measure the optical transmission through the printed PDLC droplets. A continuous wave He-Ne laser ( $\lambda = 632.8$  nm) with a 150 mm focal length lens was used to illuminate a single PDLC pixel. A neutral density filter was used to adjust the intensity of the laser. A function generator (Tektronix) coupled to a  $10\times$  voltage amplifier was used to apply an input signal to the PDLC device. A photodiode positioned at  $\approx 100$  mm distance was used to record light transmission through the printed PDLC pixel. For angle dependent scattering measurements, a 25 mm focal length imaging lens and a photodiode were mounted on a rotation stage. The stage was rotated over angles ranging from  $-45^\circ$  to  $+45^\circ$ .

### Supporting Information

Supporting Information is available from the Wiley Online Library or from the author.

### Acknowledgements

W.K. acknowledges the financial support provided by Punjab Educational Endowment Fund (PEEF), Pakistan. E.P. acknowledges the Engineering

and Physical Sciences Research Council (UK) (No. EP/M50659X/1) and Merck for financial support through a CASE studentship. S.M.M., S.J.E., J.D.L., and A.C.P. acknowledge the Engineering and Physical Sciences Research Council (UK) for financial support through the Project No. EP/R511742/1, and the John Fell Fund (Oxford University Press) through the Project No. 0005176 to provide matching funds to acquire the JetLab II system.

## Conflict of Interest

The authors declare no conflict of interest.

## Data Availability Statement

The data that supports the findings of this study are available in the supplementary material of this article.

## Keywords

drop-on-demand, inkjet printing, polymer dispersed liquid crystals, smart windows

Received: August 20, 2021

Revised: September 23, 2021

Published online: December 11, 2021

- [1] G. De Filipo, F. P. Nicoletta, G. Chid ichimo, *Adv. Mater.* **2005**, 17, 1150.
- [2] C. Zhang, Z. Guo, X. Zheng, X. Zhao, H. Wang, F. Liang, S. Guan, Y. Wang, Y. Zhao, A. Chen, G. Zhu, Z. L. Wang, *Adv. Mater.* **2020**, 32, 1904988.
- [3] C. M. Lampert, *Sol. Energy Mater. Sol. Cells* **2003**, 76, 489.
- [4] Y. J. Liu, X. W. Sun, *Adv. Optoelectron.* **2008**, 2008, 684349.
- [5] A. Ghosh, T. K. Mallick, *Sol. Energy Mater. Sol. Cells* **2018**, 176, 391.
- [6] V. K. Thakur, G. Ding, J. Ma, P. S. Lee, X. Lu, *Adv. Mater.* **2012**, 24, 4071.
- [7] P. R. Somani, S. Radhakrishnan, *Mater. Chem. Phys.* **2003**, 77, 117.
- [8] J. Lanzo, F. P. Nicoletta, G. De Filipo, G. Chidichimo, *J. Appl. Phys.* **2002**, 92, 4271.
- [9] J. L. West, *Mol. Cryst. Liq. Cryst. Inc. Nonlin. Opt.* **1988**, 157, 427.
- [10] G. P. Crawford, S. Žumer, *Liquid Crystals in Complex Geometries: Formed by Polymer and Porous Networks*, CRC Press, Taylor & Francis Group, London **1996**.
- [11] S. Bronnikov, S. Kostromin, V. Zuev, *J. Macromol. Sci., Part B* **2013**, 52, 1718.
- [12] H. M. J. Boots, J. G. Kloosterboer, C. Serbutoviez, F. J. Touwslager, *Macromolecules* **1996**, 29, 7683.
- [13] S. Pagidi, R. Manda, S. S. Bhattacharyya, S. G. Lee, S. M. Song, Y. J. Lim, J. H. Lee, S. H. Lee, *Adv. Mater. Interfaces* **2019**, 6, 1900841.
- [14] H. Ren, Y.-H. Lin, Y.-H. Fan, S.-T. Wu, *Appl. Phys. Lett.* **2005**, 86, 141110.
- [15] N. Nasir, H. Hong, M. A. Rehman, S. Kumar, Y. Seo, *RSC Adv.* **2020**, 10, 32225.
- [16] H. Ren, Y.-H. Fan, S.-T. Wu, *Appl. Phys. Lett.* **2003**, 83, 1515.
- [17] H. Ren, S.-T. Wu, *Appl. Phys. Lett.* **2002**, 81, 3537.
- [18] L. V. Natarajan, C. K. Shepherd, D. M. Brandelik, R. L. Sutherland, S. Chandra, V. P. Tondiglia, D. Tomlin, T. J. Bunning, *Chem. Mater.* **2003**, 15, 2477.
- [19] R. L. Sutherland, L. V. Natarajan, V. P. Tondiglia, T. J. Bunning, *Chem. Mater.* **1993**, 5, 1533.
- [20] T. Ishinabe, Y. Horii, Y. Shibata, H. Fujikake, *Opt. Express* **2019**, 27, 13416.
- [21] M. Kim, K. J. Park, S. Seok, J. M. Ok, H.-T. Jung, J. Choe, D. H. Kim, *ACS Appl. Mater. Interfaces* **2015**, 7, 17904.
- [22] J. E. Jung, G. H. Lee, J. E. Jang, K. Y. Hwang, F. Ahmad, J. Muhammad, J. W. Lee, Y. J. Jeon, *Opt. Mater.* **2011**, 34, 256.
- [23] J. Qi, G. P. Crawford, *Displays* **2004**, 25, 177.
- [24] M. H. Saeed, S. Zhang, Y. Cao, L. Zhou, J. Hu, I. Muhammad, J. Xiao, L. Zhang, H. Yang, *Molecules* **2020**, 25, 5510.
- [25] J. Wang, J. Xia, S. W. Hong, F. Qiu, Y. Yang, Z. Lin, *Langmuir* **2007**, 23, 7411.
- [26] J. Zou, J. Fang, *J. Mater. Chem.* **2011**, 21, 9149.
- [27] B. Derby, *Engineering* **2015**, 1, 113.
- [28] P. Calvert, *Chem. Mater.* **2001**, 13, 3299.
- [29] K. V. Wong, A. Hernandez, *ISRN Mech. Eng.* **2012**, 2012, 208760.
- [30] J. R. Castrejón-Pita, W. R. S. Baxter, J. Morgan, S. Temple, G. D. Martin, I. M. Hutchings, *At. Sprays* **2013**, 23, 571.
- [31] B. Derby, *J. Eur. Ceram. Soc.* **2011**, 31, 2543.
- [32] X. Peng, J. Yuan, S. Shen, M. Gao, A. S. R. Chesman, H. Yin, J. Cheng, Q. Zhang, D. Angmo, *Adv. Funct. Mater.* **2017**, 27, 1703704.
- [33] P. C. Duineveld, M. M. de Kok, M. Buechel, A. Sempel, K. A. H. Mutsaers, P. van de Weijer, I. G. J. Camps, T. van de Biggelaar, J.-E. J. M. Rubingh, E. I. Haskal, *Proc. SPIE* **2002**, 4464, <https://doi.org/10.1117/12.457460>.
- [34] J. Lee, D. H. Kim, J.-Y. Kim, B. Yoo, J. W. Chung, J.-I. Park, B.-L. Lee, J. Y. Jung, J. S. Park, B. Koo, S. Im, J. W. Kim, B. Song, M.-H. Jung, J. E. Jang, Y. W. Jin, S.-Y. Lee, *Adv. Mater.* **2013**, 25, 5886.
- [35] R. D. Boehm, P. R. Miller, J. Daniels, S. Stafslie, R. J. Narayan, *Mater. Today* **2014**, 17, 247.
- [36] V. J. Aliño, K. X. Tay, S. A. Khan, K. L. Yang, *Langmuir* **2012**, 28, 14540.
- [37] D. J. Gardiner, W. K. Hsiao, S. M. Morris, P. J. W. Hands, T. D. Wilkinson, I. M. Hutchings, H. J. Coles, *Soft Matter* **2012**, 8, 9977.
- [38] W. Kamal, J. Lin, S. J. Elston, T. Ali, A. A. Castrejón-Pita, S. M. Morris, *Adv. Mater. Interfaces* **2020**, 7, 2000578.
- [39] E. Parry, S. Bolis, S. J. Elston, A. A. Castrejón-Pita, S. M. Morris, *Adv. Eng. Mater.* **2018**, 20, 1700774.
- [40] J. Li, G. Baird, Y.-H. Lin, H. Ren, S.-T. Wu, *J. Soc. Inf. Disp.* **2005**, 13, 1017.
- [41] Y. Liu, B. Derby, *Phys. Fluids* **2019**, 31, 032004.
- [42] B. Derby, *Annu. Rev. Mater. Res.* **2010**, 40, 395.
- [43] C. Josserand, S. T. Thoroddsen, *Annu. Rev. Fluid Mech.* **2016**, 48, 365.
- [44] H. Wijshoff, *Phys. Rep.* **2010**, 491, 77.
- [45] Y. Kim, D. Jung, S. Jeong, K. Kim, W. Choi, Y. Seo, *Curr. Appl. Phys.* **2015**, 15, 292.
- [46] F. Ahmad, M. Jamil, J. W. Lee, S. R. Kim, Y. J. Jeon, *Electron. Mater. Lett.* **2016**, 12, 685.
- [47] M. Ellahi, F. Liu, P. Song, Y. Gao, M. Y. Rafique, D. F. Khan, H. Cao, H. Yang, *Soft Mater.* **2014**, 12, 339.
- [48] X. Dai, Y. Deng, X. Peng, Y. Jin, *Adv. Mater.* **2017**, 29, 1607022.
- [49] M. K. Choi, J. Yang, K. Kang, D. C. Kim, C. Choi, C. Park, S. J. Kim, S. I. Chae, T.-H. Kim, J. H. Kim, T. Hyeon, D.-H. Kim, *Nat. Commun.* **2015**, 6, 7149.